Electronic Supplementary Material (ESI) for Catalysis Science & Technology.

`

Supporting Information

Determining the potential-dependent identity of methane adsorbates at Pt electrodes using EC-MS

Christine Lucky,[a‡] Lee Fuller,[b‡] and Marcel Schreier[a,b]*

[a] Department of Chemical and Biological Engineering, University of Wisconsin – Madison, Madison, WI 53706, United States

[b] Department of Chemistry, University of Wisconsin – Madison, Madison, WI 53706, United States

‡These authors contributed equally.

*Correspondence: mschreier2@wisc.edu

Table of Contents

1. Supplemental Figures and Tables 2
2. Experimental Procedures
    2.1 Materials 10
    2.2 Calibration on in-situ electrochemical mass spectrometry 11
    2.3 Potentiodynamic experiments 12
    2.4 Data analysis 13
3. References 13

`

1. Supplemental Figures and Tables

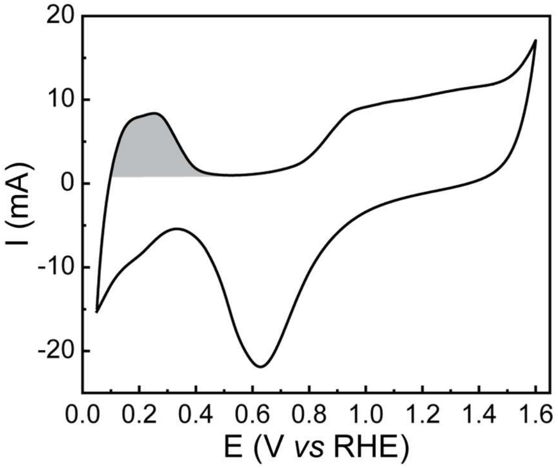

Figure S1. Sample electrochemically active surface area (ECSA) measurement where the shaded part of the CV is the region integrated to determine the ECSA of nanoporous Pt deposited onto a Pt stub. Details of the experiment are outlined in Section 2.1. The results of three separate ECSA measurements, giving an average of 147 cm^2, are shown in Table S1.

`

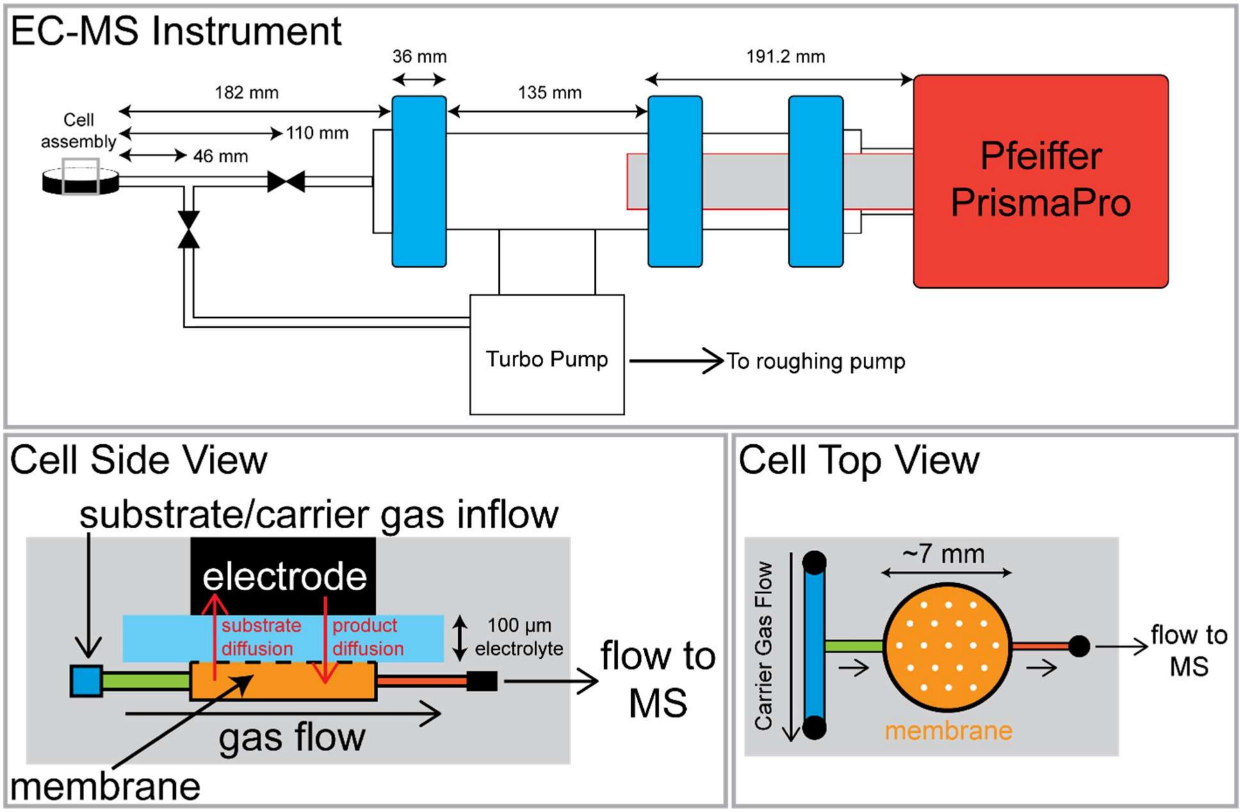

Figure S2. Schematic of EC-MS instrument and cell.

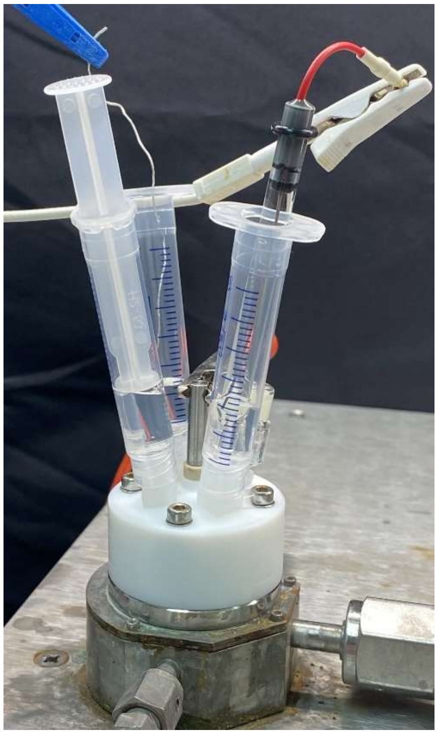

Figure S3. Photograph of the electrochemical cell mounted onto EC-MS instrument.

`

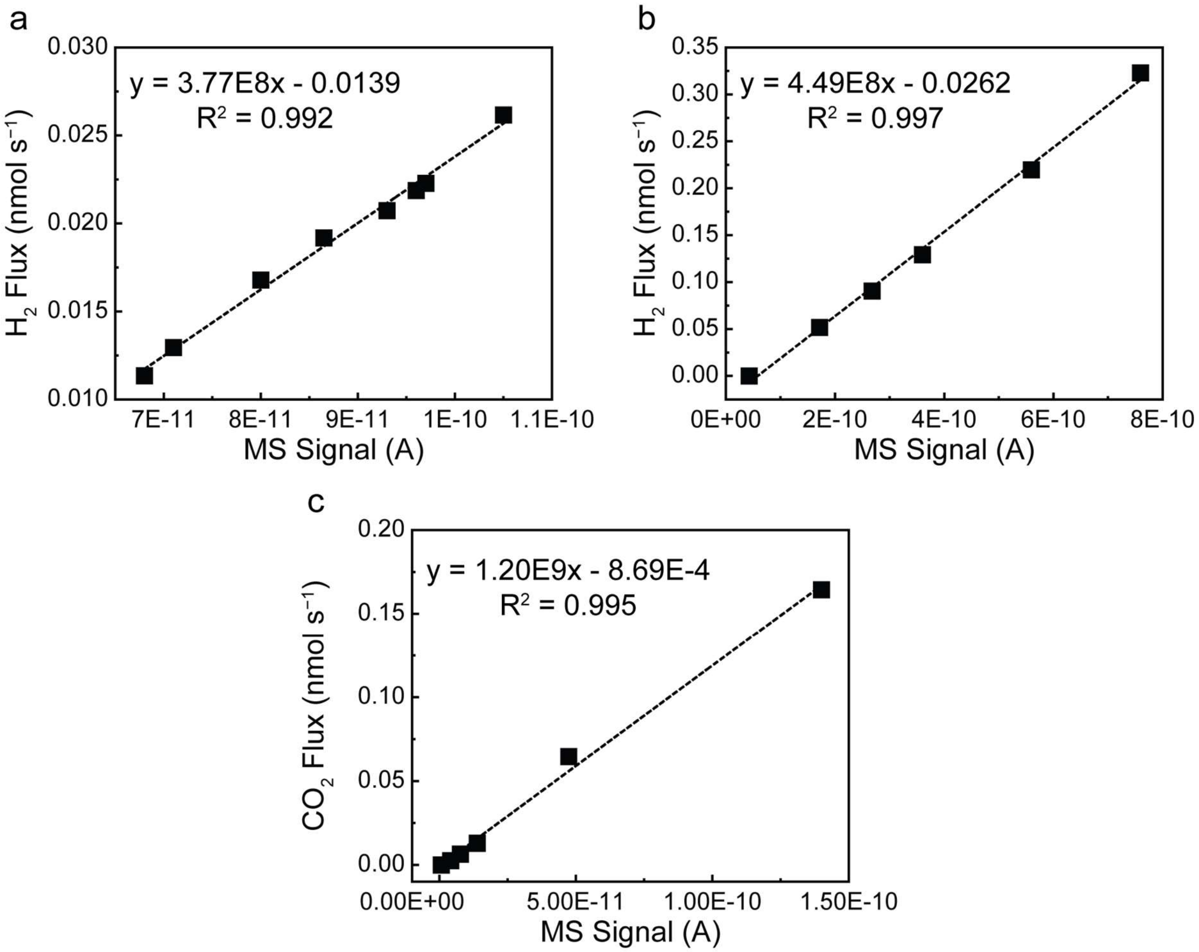

Figure S4. EC-MS calibration curves used to determine the total amount of CO_2 produced in each of the potentiodynamic experiments. Details on the calibration are given in Section 2.2. **(a)** H_2 internal calibration, **(b)** H_2 external calibration, and **(c)** CO_2 external calibration.

`

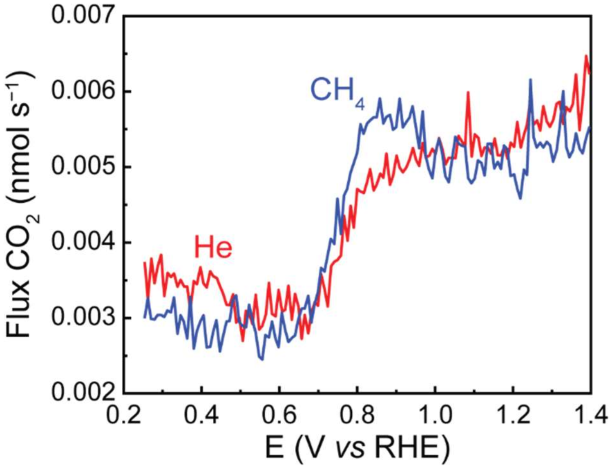

Figure S5. EC-MS quantification of CO_2 during continuous CV cycles performed under either He (red) or CH_4 (blue). Without performing a potentiostatic adsorption step, only small amounts of methane adsorb and analysis of intermediates is difficult.

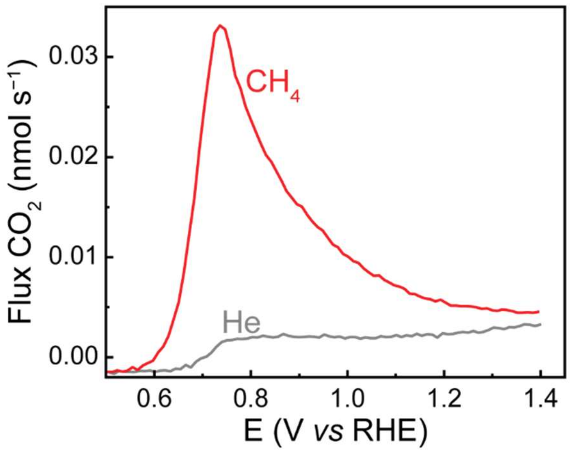

Figure S6. Flux of CO_2 produced during oxidative stripping following the adsorption of methane at 0.4 V *vs* RHE (red) or the same potential program performed under an inert helium atmosphere (gray).

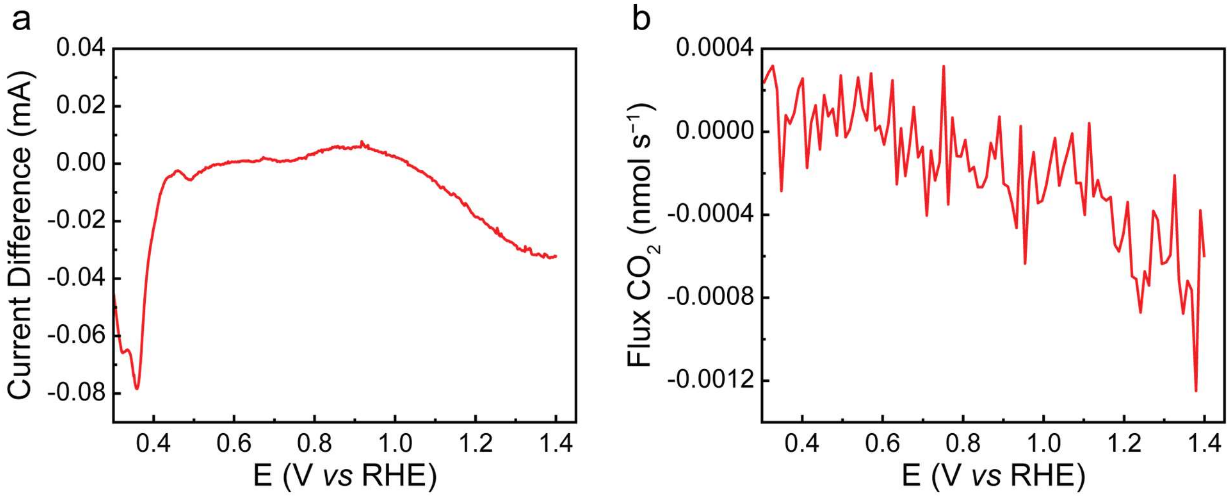

Figure S7. (a) Current difference between second cycle of methane oxidation CV and second cycle of He background CV and **(b)** flux of CO_2 produced during second cycle of CV after methane adsorption at 0.4 V *vs* RHE.

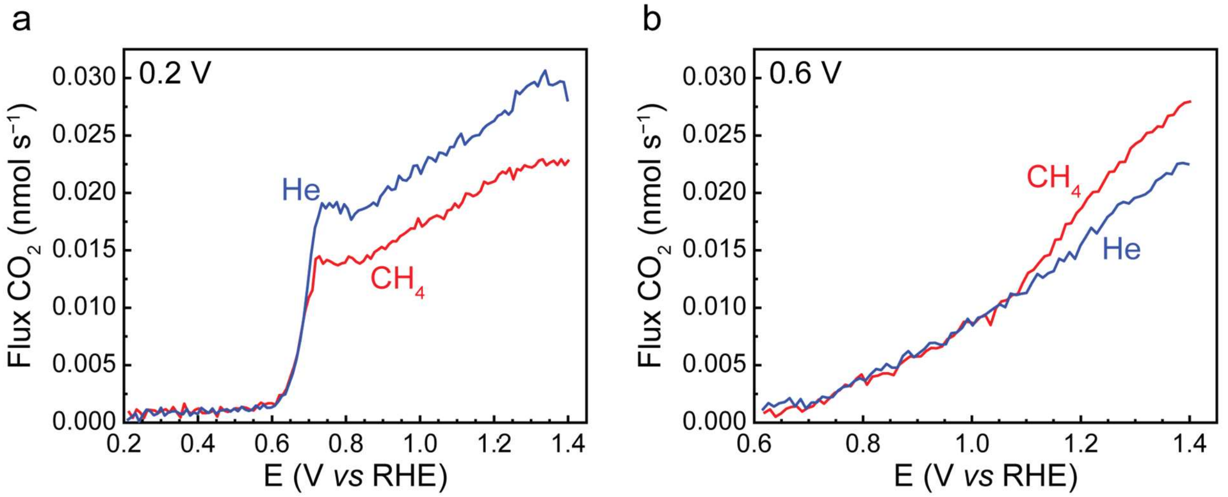

Figure S8. EC-MS quantification of CO_2 produced during oxidative stripping following methane adsorption at potentials of **(a)** 0.2 V *vs* RHE and **(b)** 0.6 V *vs* RHE.

`

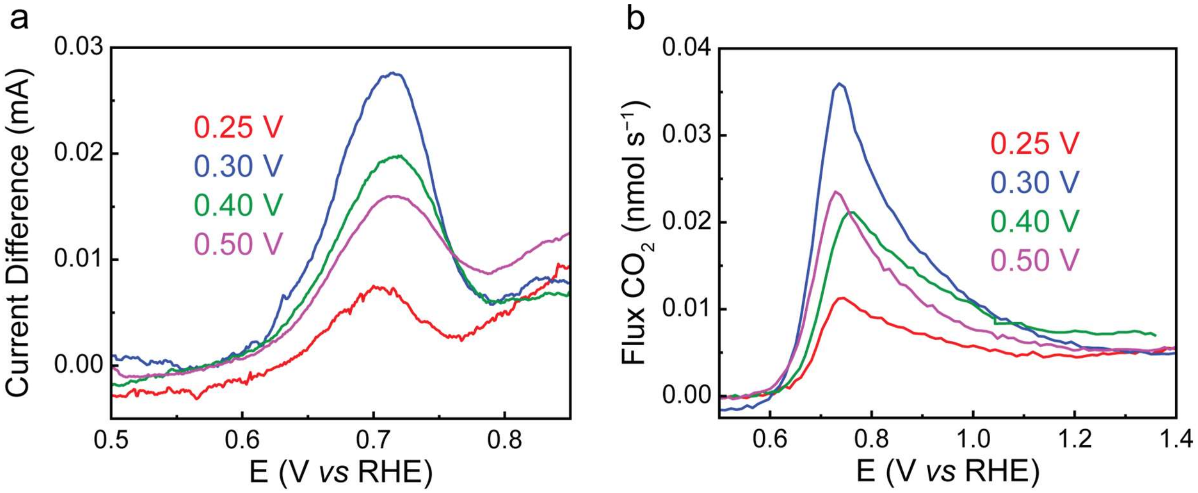

Figure S9. Representative traces for oxidative stripping following $^{12}CH_4$ adsorption at various potentials. **(a)** Voltammogram peaks that correspond to the oxidation of adsorbates, and **(b)** EC-MS quantification of CO_2 produced upon adsorbate oxidation.

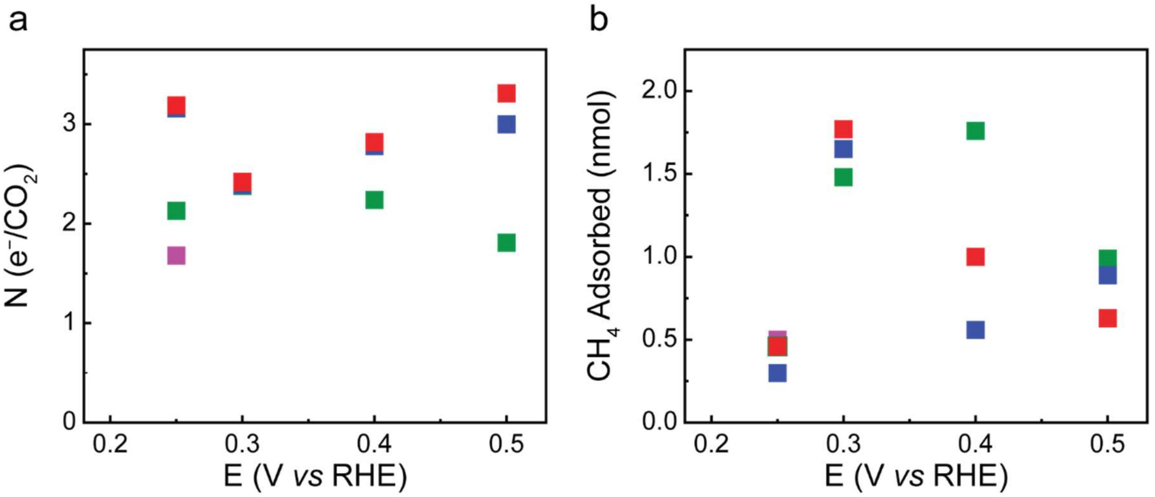

Figure S10. Replicates of potentiodynamic experiments performed under $^{12}CH_4$ at various adsorption potentials. **(a)** *N* values at each adsorption potential and **(b)** the total amount of CH_4 adsorbed at each adsorption potential. Each color used above corresponds to a different replicate performed at a specific adsorption potential. The color representing an individual replicate in **(a)** matches the color of the corresponding data point in **(b)**.

`

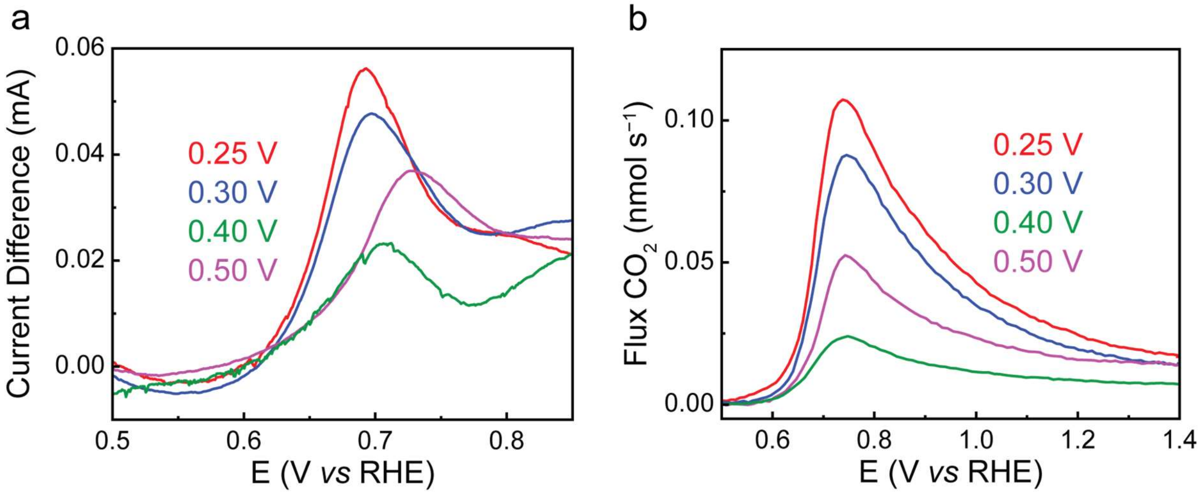

Figure S11. Representative traces for oxidative stripping following low dose CO adsorption at various potentials. **(a)** Voltammogram peaks during low dose CO experiments that correspond to the oxidation of adsorbates, and **(b)** EC-MS quantification of CO_2 produced upon adsorbate oxidation.

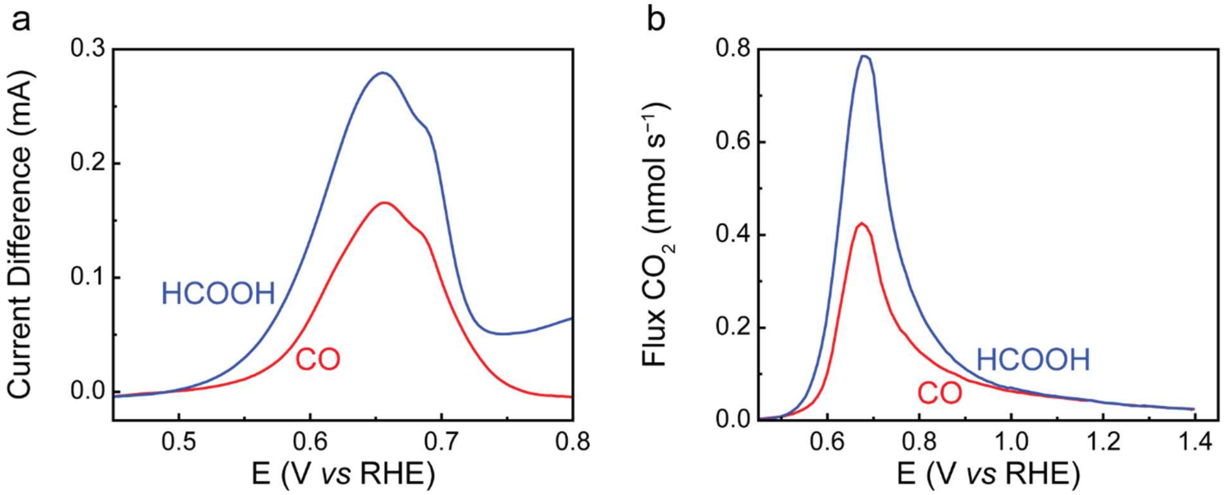

Figure S12. Potentiodynamic experiments were performed at an adsorption potential of 0.3 V *vs* RHE. ^{12}CO and formic acid (HCOOH) were used as substrates in separate experiments. ^{12}CO gave an N value of 1.69, and formic acid gave an N value of 1.70. **(a)** Voltammogram peaks that correspond to the oxidation of adsorbates, and **(b)** EC-MS quantification of CO_2 produced upon adsorbate oxidation.

`

Table S1: ECSA measurements and associated roughness factors.

Trial	ECSA (cm^2)	Roughness Factor
1	172	878
2	148	755
3	120	612
Average	147	748
Standard Deviation	21.2	109

Table S2. Individual trials of full coverage CO at 0.3 V to validate *N* method.

Trial	CO_2 Produced (nmol)	Charge Passed (mC)	*N*
1	182.61	35.05	1.99
2	202.52	41.64	2.13
3	205.33	42.00	2.12
Average	196.82	39.56	2.08
Standard Deviation	10.11	3.195	0.06

Supplementary Note S1. *N* value upper and lower bounds

The *N* values from our $^{12}CH_4$ experiments are higher than 2, meaning that there is a possibility that adsorbates other than *CO exist on the surface. Considering this, we calculate the lower and upper bounds of the fractional surface coverage of *CO at an adsorption potential of 0.3 V as follows.

For the lower bound, we consider having only *CO (N = 2) and *CHO (N = 3) present on the surface. Consider the following equation:

$$N = x_i(N_i) + x_j(N_j)$$

where $\boldsymbol{x_i}$ and $\boldsymbol{x_j}$ are the fractional surface coverages of adsorbates *i* and *j*, and N_i and N_j are the theoretical *N* values corresponding to the oxidation of *i* and *j* to CO_2. Now, we plug in for *CO, *CHO, and our experimentally calculated *N* value of 2.4:

$$2.4 = x_{CO}(2) + x_{CHO}(3)$$

Since we assume that only *CO and *CHO are present on the surface:

$$x_{CO} + x_{CHO} = 1$$

`

Now, we substitute and rearrange to solve for x_{CO} and x_{CHO}:

$$2.4 = x_{CO}(2) + (1 - x_{CO})(3)$$

$$x_{co} = 0.6, x_{CHO} = 0.4$$

As derived above, the lower bound *CO coverage for N = 2.4 gives a surface consisting of 60% *CO and 40% *CHO.

Similarly, for the upper bound, we consider having only *CO (N = 2) and *CH_2 (N = 6) present on the surface through the following treatment:

$$2.4 = x_{CO}(2) + x_{CH_2}(6)$$

$$2.4 = x_{CO}(2) + (1 - x_{CO})(6)$$

$$x_{co} = 0.9, x_{CH_2} = 0.1$$

As derived above, the upper bound for N = 2.4 gives a surface consisting of 90% *CO and 10% *CH_2.

2. Experimental Procedures

2.1 Materials

Electrolyte

All water used for cleaning and electrolyte preparation in this study was purified in a Milli-Q Reference A+ System (MilliporeSigma) to give a resistivity of 18.2 MΩ. A 1 M $HClO_4$ electrolyte prepared from 70% $HClO_4$ (99.999% trace metals basis, Sigma Aldrich) was used for all experiments.

Gases

Helium gas (Ultra High Purity Grade Helium, Airgas) was used to purge all electrolytes before experiments and was used during experiments. Methane ($^{12}CH_4$, Ultra High Purity Grade Methane, Airgas), labeled methane ($^{13}CH_4$, CO-Purified Methane, ^{13}C, 99%, Cambridge Isotope Laboratories, inc.), and carbon monoxide (^{12}CO, Research Plus, Airgas) were used as substrates. Carbon dioxide ($^{12}CO_2$, Instrument Grade, Airgas) and hydrogen (H_2, Ultra High Purity Grade Hydrogen, Airgas) were also used for calibration.

Cell Preparation

Prior to experiments, electrochemical cells were cleaned in piranha solution (75% H_2SO_4 and 25% H_2O_2) to remove organic impurities, and then thoroughly rinsed in Milli-Q water.

Catalyst Preparation

All experiments were performed using a nanoporous Pt catalyst deposited onto a Pt stub (99.995%, Pine Instruments). The deposition protocol is adapted from a previous work.[1] A Pt stub

`

was polished in 0.3 μm alumina suspension (Allied High Tech Products) and rinsed thoroughly in Milli-Q water. Following this, the surface of the Pt stub was placed into contact with an aqueous solution consisting of 72 mM H_2PtCl_6 (99.9% trace metals basis, Sigma Aldrich) and 0.13 mM $Pb(C_2H_3O_2)_2$ (99.999% trace metals basis, Sigma Aldrich). Using a Biologic SP-200 potentiostat and a Pt wire (99.99%, Kurt J. Lesker Company) as the counter electrode, a constant current of -10 mA/cm^2 was applied to the Pt stub for 10 minutes. After electrodeposition, the Pt stub was gently rinsed in Milli-Q water before use.

Catalyst Characterization

The electrochemical surface area (ECSA) of the electrodeposited Pt stub was calculated by adapting a method from a previous work.[2] The electrodeposited Pt stub was placed into contact with a solution of 1 M $HClO_4$. Pt wire was used as the counter electrode and Ag/AgCl (3 M KCl, BASi) was used as the reference electrode.

While flowing He into the electrolyte, a Gamry Interface 1010E potentiostat was used to apply a constant potential of 1.3 V *vs* RHE to the electrodeposited Pt stub for 1 minute. After this, from an initial potential of 1.3 V *vs* RHE, CV was performed and the potential was swept positively at a scan rate of 50 mV s^{-1}. The vertex potentials of the CV were 1.6 V *vs* RHE and –0.05 V *vs* RHE. 5 complete CV cycles were performed before the measurement ended at 0.05 V *vs* RHE. From there, CV was performed again at a scan rate of 50 mV/s. The vertex potentials of the CV were 0.05 V *vs* RHE and 1.6 V *vs* RHE. The 10th cycle of the CV was used to calculate the ECSA. The hydrogen under potential deposition region of the CV was integrated (**Figure S1**) to give the charge passed and converted to ECSA using a value of 210 μC/cm^2.[2]

Scanning electron microscopy was used to image the electrodeposited Pt stub. Imaging was performed with a Zeiss GeminiSEM 450, operating at an acceleration voltage of 3.00 kV with an InLens detector.

2.2 Calibration of in-situ electrochemical mass spectrometry

Electrocatalytic experiments were conducted using an EC-MS system (SpectroInlets, Denmark) controlled by Zillien software (SpectroInlets, Denmark). The experiments were performed in a PTFE electrochemical cell placed on top of a semipermeable membrane chip (SpectroInlets, Denmark) that allows diffusion of gaseous products through the chip and into the MS for analysis. The working principle of this system has been published elsewhere.[3]

A two-step procedure consisting of an internal and external calibration was performed to quantify the products generated during these experiments. For the internal calibration, the hydrogen evolution reaction (HER) was performed since this reaction can be carried out at 100% Faradaic efficiency (FE), and the EC-MS system theoretically allows 100% of desorbed products to be collected and analyzed.

To perform the internal calibration, a polished Pt stub was put into contact with 1 M $HClO_4$, and a series of constantly reductive currents was applied to the Pt stub until the resulting H_2 signal (m/z 2) stabilized. Since HER occurs at 100% FE, the theoretical production rate of H_2 (nmol/s) at each applied current was calculated and related to the magnitude of the m/z 2 ionic current (A). This allowed the generation of an internal H_2 calibration curve.

Products besides hydrogen are not necessarily produced with 100% FE, and therefore must be calibrated externally. External calibrations were performed by flowing known concentrations of dilute analyte gases into the EC-MS system and recording the corresponding MS signals. Gas

`

dilution was accomplished by mixing the analyte gas with He using six mass flow controllers (Alicat). The collection efficiency of He was determined by performing an external hydrogen calibration. The stable m/z 2 signals resulting from flowing various concentrations of dilute H_2 into the EC-MS system were compared to the internal HER calibration, and H_2 flux vs gas concentration data was generated for the dilute regime. By assuming that the flux of He is constant to within 0.5 mol %, calculation of the total flux of gas through the chip capillary was accomplished using the equation below:

$$He\, flux\, into\, MS\ =\ \frac{(H_2\, signal\ -\ b)/m}{x_{H_2}}$$

where b is the internal HER calibration fit's intercept, m is its slope, and x_{H_2} is the mole fraction of H_2.

The flux of diluted analyte gas to the MS was determined for other species by assuming the flux of the diluent (He) is constant. Hydrogen, methane, and $^{12}CO_2$ were calibrated to m/z 2, m/z 15, and m/z 44 respectively. The corresponding calibration curves are shown in **Figure S3**.

2.3 Potentiodynamic experiments

Potentiodynamic experiments were performed using He and various substrates, including $^{12}CH_4$, $^{13}CH_4$, and ^{12}CO. The prepared nanoporous Pt catalyst was placed into a PTFE cell and mounted onto the EC-MS system. 1 M $HClO_4$ was used as the electrolyte, Pt wire was used as the counter electrode, and Ag/AgCl was used as the reference electrode. Experiments were performed using a Biologic SP-200 potentiostat in series with a decade box to increase stability. Between the potentiostat and working electrode connection of the electrochemical cell, the decade box was set to a resistance of 100 Ω. Under He flow at 1 mL min^{-1}, potentio electrochemical impedance spectroscopy was performed (PEIS) at open circuit potential (OCP). Following that, a potential of 1.3 V *vs* RHE was applied for 1 minute to clean the electrode surface. After this, the electrode was conditioned by performing CV. From 1.3 V *vs* RHE, the potential was swept positively at a scan rate of 50 mV s^{-1}, with vertex potentials of 1.4 V and –0.05 V *vs* RHE. 5 total cycles were performed, and the scan ended at the adsorption potential of that specific experiment (either 0.25 V, 0.3 V, 0.4 V, or 0.5 V *vs* RHE).

Starting at the adsorption potential, two identical He background experiments consisting of chronoamperometry and CV were performed. The background experiment is as follows: While still flowing He at 1 mL/min, the adsorption potential of the experiment (either 0.25 V, 0.3 V, 0.4 V, or 0.5 V *vs* RHE) was applied for 30 minutes. Then, the potential was swept positively at a scan rate of 5 mV s^{-1} using CV. The vertex potentials were 1.4 V and 0.05 V *vs* RHE, and a total of 3 cycles were performed. The last scan of the CV ended at the adsorption potential of the experiment. After this, an identical He background experiment was performed, once again ending at the adsorption potential of the experiment. For $H^{12}COOH$ experiments, from t = 15 minutes to t = 18 minutes of the potential hold for the second He background experiment, 1 M $HClO_4$ was flowed through the system at a flow rate of 2 mL min^{-1}. After t = 18 minutes, flowing was halted.

Following the He background experiments, the adsorption potential was applied for 30 minutes, and the substrate ($^{12}CH_4$, $^{13}CH_4$, ^{12}CO, $H^{12}COOH$) used for the experiment was introduced into the system. For experiments using $^{12}CH_4$ and $^{13}CH_4$, these gases were flowed into the system at 1 mL min^{-1} for the first 15 minutes of the adsorption potential hold. From there, He

`

was flowed into the system for 10 minutes at 14 mL min^{-1}, and then changed to a flow rate of 1 mL min^{-1} for the last 5 minutes of the adsorption potential hold. As for ^{12}CO, this gas was flowed into the system at 1 mL min^{-1} for 1 minute. From there, He was flowed into the system for 10 minutes at 14 mL min^{-1}, followed by 1 mL/min for the remainder of the adsorption potential hold. In **Figure S12**, ^{12}CO was flowed into the system for about 1.3 mins to give similar CO_2 flux as in 0.001 M HCOOH. For H^{12}COOH, at the end of the second He background experiment, the potential was set to the open-circuit voltage for 3.5 minutes. During this time, 0.001 M H^{12}COOH (dissolved in 1 M $HClO_4$) was flowed into the EC-MS cell at 2 mL min^{-1}. Following this, flowing was halted and the adsorption potential was applied for 30 minutes. After the first 15 minutes of the adsorption potential hold, 1 M $HClO_4$ was flowed into the electrochemical cell for 3 minutes at a rate of 2 mL min^{-1} to remove non-adsorbed H^{12}COOH.

At the end of the adsorption potential hold, the potential was swept positively at a scan rate of 5 mV s^{-1} by using CV. The vertex potentials were 1.4 V and 0.05 V *vs* RHE, and a total of 3 cycles were performed. The last scan ended at the adsorption potential of experiment.

2.4 Data analysis

Oxidation of the substrate to CO_2 is convoluted by oxidation of unknown organic impurities to CO_2. For this reason, *N* values were calculated using background subtractions to remove contributions from organic impurities. The peak of the CV representing the oxidation of substrate from the surface ($^{12}CH_4$, $^{13}CH_4$, or ^{12}CO) was subtracted by the first scan of the second He background experiment, removing the charge associated with the oxidation of organic impurities. In addition, the flux of CO_2 produced when oxidizing the substrate ($^{12}CH_4$ or ^{12}CO) was subtracted by the flux of CO_2 produced during the first scan of the second He background experiment, removing the flux of CO_2 associated with the oxidation of organic impurities. When $^{13}CH_4$ was used as the substrate, background subtraction of the flux was not performed since it is oxidized to $^{13}CO_2$ (m/z 45), which is distinguishable from $^{12}CO_2$ (m/z 44) originating from organic impurities.

References

(1) Feltham, A. M.; Spiro, M. Platinized platinum electrodes. *Chem. Rev.* 1971, 71, 177-193.

(2) Boyd, M. J.; Latimer, A. A.; Dickens, C. F.; Nielander, A. C.; Hahn, C.; Norskov, J. K.; Higgins, D. C.; Jaramillo, T. F. Electro-Oxidation of Methane on Platinum under Ambient Conditions. *ACS Catal.* 2019, *9* (8), 7578–7587.

(3) Trimarco, D. B.; Scott, S. B.; Thilsted, A. H.; Pan, J. Y.; Pedersen, T.; Hansen, O.; Chorkendorff, I.; Vesborg, P. C. K. Enabling Real-Time Detection of Electrochemical Desorption Phenomena with Sub-Monolayer Sensitivity. *Electrochim. Acta* 2018, *268*, 520–530.